Spin-Wave Excitation in Magnetic Insulators by Spin-Transfer Torque

Jiang Xiao (萧江)

Department of Physics and State Key Laboratory of Surface Physics, Fudan University, Shanghai 200433, China

Gerrit E. W. Bauer

Institute for Materials Research, Tohoku University, Sendai 980-8557, Japan
Kavli Institute of NanoScience, Delft University of Technology, 2628 CJ Delft, The Netherlands

We study the excitation of spin waves in magnetic insulators by the current-induced spin-transfer torque. We predict preferential excitation of surface spin waves induced by an easy-axis surface anisotropy with critical current inversely proportional to the penetration depth and surface anisotropy. The surface modes strongly reduce the critical current and enhance the excitation power of the current-induced magnetization dynamics.

PACS numbers: 85.75.−d, 75.30.Ds, 75.76.+j

Spintronics is all about manipulation and transport of the spin, the intrinsic angular momentum of the electron [1]. These two tasks are incompatible, since manipulation requires strong coupling of the spin with the outside world, which perturbs transport over long distances. In normal metals, spin can be injected and read out easily, but the spin information is lost over short distances [2]. In spin-based interconnects, transporting spins over longer distances is highly desirable [3].

The long-range transport of spin information can be achieved by encoding the information into spin waves that are known to propagate coherently over centimeters [4]. It has been demonstrated in Refs. [5–7] for the magnetic insulator Yttrium-Iron-Garnet (YIG) that spin waves can be actuated electrically by the spin-transfer torque [8,9] and detected by spin pumping [10] at a distant contact. In the experiment by Kajiwara [5], Pt was used as spin current injector and detector, making use of the (inverse) spin Hall effect [11]. In a $d = 1.3$ μm-thick YIG film, spin waves were excited by a threshold charge current of $J_c \sim 10^9$ A/m^2. This value is much less than expected for the bulk excitation that in a linear approximation corresponds to the macrospin mode and is estimated as $J_c = (1/\theta_H)e\alpha\omega M_s d/\gamma\hbar \sim 10^{11\sim12}$ A/m^2, where e and γ are the electron charge and gyromagnetic ratio, respectively, and we used the parameter values in Table I for the ferromagnetic resonance frequency ω, the spin Hall angle of Pt θ_H, magnetic damping α, and saturation magnetization M_s. In this estimate we disregarded any incomplete absorption of the transverse spin current based on recent insights on the interface of the YIG with normal metals [14,15].

In this Letter, we address this large mismatch between observed and expected critical currents by studying the threshold current and excitation power of current-induced spin wave excitations. We present a possible answer to the conundrum by proving that the threshold current is strongly decreased in the presence of an easy-axis surface anisotropy (EASA). Simultaneously, EASA increases the power of the spin wave excitation by at least two orders of magnitude.

We study a structure as depicted in Fig. 1, where a nonmagnetic (N) metallic thin film of thickness t is in contact with a ferromagnetic insulator (FI), whose equilibrium magnetization is along the z direction. The spin current injected into the ferromagnetic insulator is polarized transverse to the magnetization $\mathbf{J}_s = J_s\mathbf{m} \times \hat{\mathbf{z}} \times \mathbf{m}$. The bulk magnetization is described by the Landau-Lifshitz-Gilbert (LLG) equation:

$$\dot{\mathbf{m}} = -\gamma\mathbf{m} \times [\mathbf{H}_0 + (A_{\mathrm{ex}}/\gamma)\nabla^2\mathbf{m} + \mathbf{h}] + \alpha\mathbf{m} \times \dot{\mathbf{m}}, \quad (1)$$

where $\mathbf{H}_0$ includes the external and internal magnetic field, A_{ex} is the exchange constant, $\mathbf{h}$ is the dipolar field that satisfies Maxwell's equations, and α is the total effective damping parameter. The damping caused by the 2-magnon processes in ultrathin ferromagnets [16] is assumed to be constant within the small frequency range of interest. In the quasistatic approximation, i.e., disregarding retardation in the electromagnetic waves, $\nabla \times \mathbf{h} = 0$ and $\nabla \cdot \mathbf{b} = \nabla \cdot (\mathbf{h} + \mu_0 M_s\mathbf{m}) = 0$. All quantities are position- and

TABLE I. Parameters for YIG.

Parameter	YIG	Unit
γ	1.76×10^{11}	1/(Ts)
M_s	[a]1.56×10^5	A/m
$\omega_M = \gamma\mu_0 M_s$	34.5	GHz
A_{ex}	4.74×10^{-6}	m^2/s
α	6.7×10^{-5}	$\cdots$
$\omega_0 = \gamma H_0$	$0.5\omega_M$	GHz
K_s	[b]5×10^{-5}	J/m^2

[a]Ref. [5].
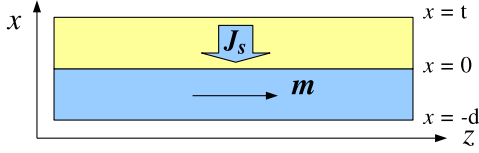[b]K_s ranges 0.01–0.1 erg/cm^2 or $10^{-5}10^{-4}$ J/m^2, Refs. [12,13].

FIG. 1 (color online). An electrically insulating magnetic film of thickness d with magnetization $\mathbf{m}$ ($\parallel \hat{\mathbf{z}}$ at equilibrium) in contact with a normal metal. A spin current $J_s \parallel \hat{\mathbf{z}}$ is generated in the normal metal and absorbed by the ferromagnet.

time-dependent. In the absence of pinning, the total torque vanishes at the interface [17]:

$$A_{\mathrm{ex}}\mathbf{m} \times \frac{\partial \mathbf{m}}{\partial \mathbf{n}} - \frac{2\gamma K_s}{M_s}(\mathbf{m}\cdot\mathbf{n})\mathbf{m}\times\mathbf{n} + \frac{\gamma J_s}{M_s}\mathbf{m}\times\hat{\mathbf{z}}\times\mathbf{m} = \mathbf{0},$$
$$(2)$$

where $\mathbf{n}$ is the outward normal as seen from the ferromagnet. The first term in Eq. (2) is the surface exchange torque, the second term the torque due to a perpendicular uniaxial surface anisotropy $\mathbf{H}_a = \frac{2K_1}{M_s}(\mathbf{m}\cdot\mathbf{n})\mathbf{n}$ and $K_s = \int dx K_1$ across the surface, and the last term is the current-induced spin-transfer torque [18]. We parameterize the surface anisotropy and spin current as wave numbers $k_s = 2\gamma K_s/A_{\mathrm{ex}}M_s$ and $k_j = \gamma J_s/A_{\mathrm{ex}}M_s$. The dipolar fields $h_{y,z}$ and b_x are continuous across the interface. Eqs. (1) and (2) in combination with Maxwell's equations describe the low energy magnetization dynamics and can be transformed into a sixth-order differential equation for the scalar potential ψ with $\mathbf{h} = -\nabla\psi$ [19,20].

The method described above extends previous studies by Hillebrands [20] and references therein by including the current-induced spin-transfer torque. We predict the critical conditions under which magnetization dynamics becomes amplified by the current-induced driving torque.

We start with the limiting case of $d \to \infty$ (semi-infinite ferromagnet). After linearization and Fourier transformation in both time and space domains, Eq. (1) reduces to a fourth-order differential equation in ψ. Focusing for simplicity first on the case of vanishing in-plane wave vector $\mathbf{q} = (q^y, q^z) = \mathbf{0}$, the scalar potential can be written as $\psi(\mathbf{r}) = \sum_{j=1}^{2} a_j e^{iq_j x} e^{i\omega t}$ with

$$q_j(\omega) = -i\left(\frac{\omega_0 + \frac{1}{2}\omega_M \pm \sqrt{\omega^2 + \frac{1}{4}\omega_M^2} + i\alpha\omega}{A_{\mathrm{ex}}}\right)^{1/2} \quad (3)$$

and $|q_1| \gg |q_2|$ when $\omega \sim \omega_0$. Imposing the boundary condition in Eq. (2), up to the first order in k_j:

$$0 = 2q_1 q_2(q_1 + q_2) + ik_s\left[(q_1+q_2)^2 + \frac{\omega_M}{A_{\mathrm{ex}}}\right] + 4k_j\omega. \quad (4)$$

The solutions of Eq. (4) are the *complex* eigenfrequencies ω, whose real part represents the energy and imaginary part, the inverse lifetime. To zeroth order in dissipation, i.e., with vanishing bulk damping ($\alpha = 0$) and spin current

injection ($k_j = 0$), and using $|q_1| \gg |q_2|$, Eq. (4) simplifies to $k_s = 2iq_2/[1 + \omega_M/(Aq_1^2)]$, which has no nontrivial solution for $k_s \leq 0$. The single real solution for $k_s > 0$ obeys $\omega < \sqrt{\omega_0(\omega_0 + \omega_M)}$ such that both $q_{1,2}$ are negative imaginary: $q_1 \simeq -i\sqrt{(2\omega_0 + \omega_M)/A_{\mathrm{ex}}}$, $q_2 \simeq -ik_s\omega_0/(2\omega_0 + \omega_M) + O(k_s^2)$, i.e., a surface spin wave induced by the easy-axis surface anisotropy. With the criteria $\mathrm{Im}\,\omega < 0$ and to leading order in $0 < k_s \ll q_1$, Eq. (4) leads to the critical current:

$$k_j^c \approx -\frac{\alpha}{k_s}\frac{(\omega_0 + \omega_M/2)^2}{A_{\mathrm{ex}}\omega_0} + \alpha\frac{\omega_0 + 2\omega_M}{4\omega_0}\sqrt{\frac{2\omega_0 + \omega_M}{A_{\mathrm{ex}}}}. \quad (5)$$

When there is no surface anisotropy ($k_s \to 0$), the critical current diverges because the macrospin mode cannot be excited in a semi-infinite film. Using the parameters given in Table I in Eq. (5), we estimate the critical current for exciting the EASA-induced surface wave (at $\mathbf{q} = 0$) to be $k_j^c = -0.08k_c$, where $k_c = \alpha(\omega_0 + \omega_M/2)d/A_{\mathrm{ex}}$ is the critical current for bulk excitation in a YIG thin film of thickness $d = 0.61~\mu$m (used below).

EASA pulls down a surface spin wave for the following reason: when $k_j = J_s = 0$, the boundary condition in Eq. (2) requires cancellation between the exchange and surface anisotropy torques: $\partial_x m_x - k_s m_x = \partial_x m_y = 0$. The exchange torque depends on the magnetization derivative in the normal direction and can only take one sign in the whole film, and $m_{x,y} \to 0$ as $x \to -\infty$, therefore $(1/m_x)\partial_x m_x > 0$. Torque cancellation (for a nontrivial solution) is therefore possible only for $k_s > 0$. The surface spin wave induced by EASA ($k_s > 0$) for the *in-plane* magnetized film ($m_z \sim 1$) discussed in this Letter is analogous to the surface spin waves for the *perpendicular* magnetized film ($m_x \sim 1$) induced by easy-plane surface anisotropy ($k_s < 0$) studied before in YIG films [17,21–24]. For perpendicular magnetization, a different boundary condition, $\partial_x m_{y,z} + k_s m_{y,z} = 0$, results in a surface wave for $k_s < 0$.

We now include all ingredients: finite thickness ($d = 0.61~\mu$m), surface anisotropy, intrinsic magnetic damping, spin current injection, exchange coupling, and dipolar fields. We calculate numerically the complex eigenfrequencies $\omega(\mathbf{q}, k_j)$ as a function of the in-plane wave vector $\mathbf{q}$ and the applied spin current at the surface k_j. $\mathrm{Im}\,\omega$, the effective dissipation, can be either positive (damping) or negative (amplification) when driven by the spin-transfer torque.

First, we disregard the surface anisotropy: $K_s = k_s = 0$. With θ the angle between $\mathbf{q}$ and $\mathbf{m}$, the results for $\theta = 90°$ are shown in Fig. 2. In the top left panels $\mathrm{Re}\,\omega$, the magnetostatic surface wave (MSW) is seen to cross the flat bulk bands [19]. When no spin current is applied ($k_j = 0$), the dissipative part $\mathrm{Im}\,\omega \sim \alpha(\omega_0 + \omega_M/2) > 0$, as shown in the top middle panels. At a spin current that is 20% of that required for bulk excitation: $k_j = 0.2k_c$, the
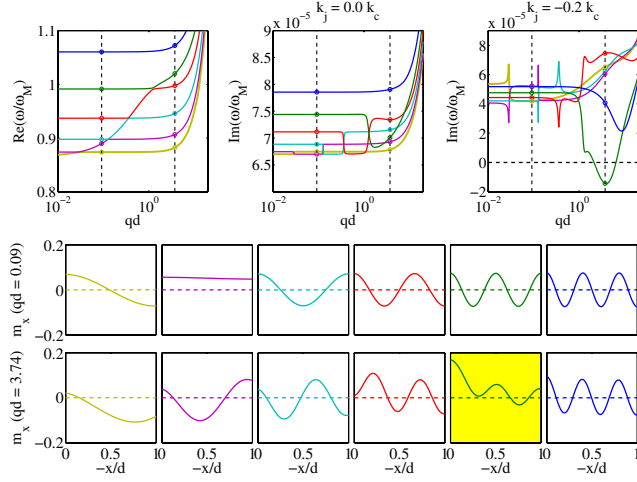
FIG. 2 (color online).   Spin wave band structure and magnetization profiles in YIG for $d = 0.61$ μm without surface anisotropy: $k_s = 0$ at $\theta = \angle(\mathbf{m}, \mathbf{q}) = 90°$. Top (from left to right): $\mathrm{Re}(\omega/\omega_M)$ vs. qd, $\mathrm{Im}(\omega/\omega_M)$ at $k_j = 0$, $\mathrm{Im}(\omega/\omega_M)$ at $k_j = -0.2k_c$. Bottom: m_x of the same 6 modes for $qd = 0.09$ and 3.74 indicated by the dashed vertical lines in the top panels. The colors label different bands. The amplitude of the green mode (shaded [yellow] panel) is amplified.

dissipative part $\mathrm{Im}\,\omega$ (top right panel) decreases while $\mathrm{Re}\,\omega$ remains unchanged because the spin-transfer torque as magnetic (anti-)damping mainly affects $\mathrm{Im}\,\omega$. Negative effective dissipation implies spin-wave amplification. This happens for the 5th (green) band at $qd \in [2, 6.5]$, which corresponds to a (chiral) MSW (mixed with bulk modes) formed near the interface (shaded [yellow] panel). On the other hand, for $\theta = -90°$ (not shown), the magnetostatic surface wave at the opposite surface to vacuum ($x = -d$) is only weakly affected by the spin current injection at $x = 0$. The peaks (dips) in the top right panel in Fig. 2 occur at the mode crossing (anticrossing) points between the bulk mode and MSW because $m_{x,y}(0)$ for the corresponding mode decrease (increase) during the crossing, thereby minimizing (maximizing) the effect of the spin-transfer torque.

We now turn on EASA: $k_s = 25.0/\mu$m (or $K_s = 5 \times 10^{-5}$ J/m^2) at the top surface ($x = 0$). Fig. 3 shows the results for $\theta = 90°$. The changes of $\mathrm{Re}\,\omega$ and $\mathrm{Im}\,\omega$ at $k_j = 0$ are modest (Fig. 2), but an additional band (black) appears, viz. the surface spin wave band induced by EASA. The spin-transfer torque strongly affects this mode because of its strong surface localization [25]. As seen in the top right panel, almost the whole band is strongly amplified by a spin current injection of $k_j = 0.2k_c$. Inspecting the spin wave profiles at two different q values, we observe a surface spin wave near $x = 0$ for the black band at small q (shaded [yellow] panel in the middle row in Fig. 3). At larger q, the 1st (black) band loses its surface wave features to the 5th (red) band (see top right panel in Fig. 3). The red band mode starts out as a magnetostatic surface spin wave,
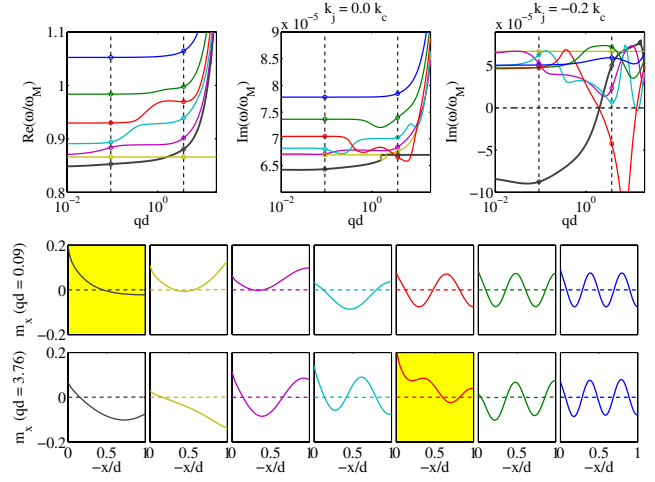

FIG. 3 (color online).   Same as Fig. 2 but with $k_s = 25/\mu$m.

but the EASA enhances its surface localization by hybridization with the black mode to become strongly amplified by the spin current at higher q. Also in the lower panel of Fig. 3, we observe that the red band has acquired the surface character.

We introduce an approximate power spectrum (Fig. 4) that summarizes all information about the mode-dependent current-induced amplification

$$P(\omega) = \sum_n \int_{\mathrm{Im}\,\omega_n < 0} |\mathrm{Im}\,\omega_n(\mathbf{q})| \delta[\omega - \mathrm{Re}\,\omega_n(\mathbf{q})] d\mathbf{q} \quad (6)$$

with n the band index is the density of states at frequency ω weighted by its amplification. $P(\omega)$ represents the frequency dependence of the excitation power but not its absolute scale. Without surface anisotropy, only a few modes are excited even at a relatively large current ($k_j = 0.2k_c$). However, when $k_s = 25/\mu$m, the excitation is strongly enhanced by more than two orders of magnitude due to the easily excitable surface spin wave modes. Furthermore, we observe broadband excitation over a
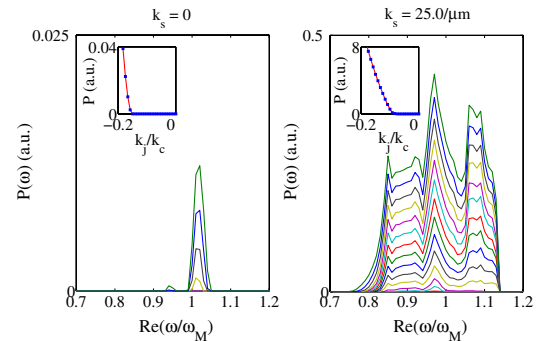

FIG. 4 (color online).   Top: Power spectrum (resolution $\delta\omega/\omega_M = 0.01$) at various current levels ($k_j = 0.2k_c$ from the top decreasing by $\Delta k_j = 0.01k_c$) without (left: $k_s = 0$) and with (right: $k_s = 25.0/\mu$m) surface anisotropy. Inset: the integrated power versus k_j.

much larger range of frequencies. This power spectrum is rather smooth, while the experiments by Kajiwara *et al.* [5] show a large number of closely spaced peaks. The latter fine structure is caused by size quantization of spin waves due to the finite lateral extension of the sample that has not been taken into account in our theory since it complicates the calculations without introducing new physics. The envelope of the experimental power spectrum compares favorably with the present model calculations.

The insets in Fig. 4 show the integrated power and allow the following conclusions: (i) the excitation power is enhanced by at least two orders of magnitude by the EASA; (ii) the critical current for magnetization dynamics is $k_j \sim -0.08 k_c$ for $k_s = 25/\mu$m, which agrees very well with the estimates from Eq. (5). This critical current is about one order of magnitude smaller than that for the bulk excitation (k_c) and about half of that for MSW without surface anisotropy ($k_j = -0.16 k_c$). For $k_s = 25/\mu$m, it corresponds to $J_c = 3 \times 10^{10}$ A/m^2 for $\theta_H = 0.01$ [26] and 3.8×10^9 A/m^2 for $\theta_H = 0.08$ [27,28]. These values are calculated for a film thickness of $d = 0.61 \mu$m but should not change much for $d = 1.3 \mu$m corresponding to the experiment [5], because the excited spin waves are localized at the interface. Compared to the original estimate $J_c \sim 10^{11}$–10^{12} A/m^2, the critical current for a surface spin wave excitation is much closer to the experimental value of $J_c \sim 10^9$ A/m^2 [5] (although these experiments report a very inefficient spin wave absorption in contrast to the present model assumption).

According to Eq. (5), critical current (excitation power) would be further reduced (increased) by a larger EASA. Reference [12] reports an enhancement of the YIG surface anisotropies for capped as compared to free surfaces. A Pt cover on a YIG surface [5] may enhance the surface anisotropy as well. As seen from Fig. 3, the surface mode (black band) has group velocity $\partial\omega/\partial\mathbf{q}$ comparable to that of the MSW. The excited surface spin wave therefore propagates and can be used to transmit spin information over long distances at a much lower energy cost than the bulk spin waves.

In conclusion, we predict that an easy-axis surface anisotropy gives rises to a surface spin wave mode, which reduces the threshold current required to excite the spin waves and dramatically increases the excitation power. Multiple spin wave modes can be excited simultaneously at different frequencies and wave vectors, thereby explaining recent experiments. Surface spin wave excitations could be useful in low-power future spintronics-magnonics hybrid circuits.

[1] I. Žutić, J. Fabian, and S. Das Sarma, Rev. Mod. Phys. **76**, 323 (2004).

[2] J. Bass and W. P. Pratt, J. Phys. Condens. Matter Lett. **19**, 183201 (2007).

[3] A. Khitun and K. L. Wang, J. Appl. Phys. **110**, 034306 (2011).

[4] A. A. Serga, A. V. Chumak, and B. Hillebrands, J. Phys. D **43**, 264002 (2010).

[5] Y. Kajiwara, K. Harii, S. Takahashi, J. Ohe, K. Uchida, M. Mizuguchi, H. Umezawa, H. Kawai, K. Ando, K. Takanashi *et al.*, Nature (London) **464**, 262 (2010).

[6] M. Madami, S. Bonetti, G. Consolo, S. Tacchi, G. Carlotti, G. Gubbiotti, F. B. Mancoff, M. A. Yar, and J. Akerman, Nature Nanotech. **6**, 635 (2011).

[7] Z. Wang, Y. Sun, M. Wu, V. Tiberkevich, and A. Slavin, Phys. Rev. Lett. **107**, 146602 (2011).

[8] J. C. Slonczewski, J. Magn. Magn. Mater. **159**, L1 (1996).

[9] L. Berger, Phys. Rev. B **54**, 9353 (1996).

[10] Y. Tserkovnyak, A. Brataas, and G. E. W. Bauer, Phys. Rev. Lett. **88**, 117601 (2002).

[11] E. Saitoh, M. Ueda, H. Miyajima, and G. Tatara, Appl. Phys. Lett. **88**, 182509 (2006).

[12] P. Yen, T. S. Stakelon, and P. E. Wigen, Phys. Rev. B **19**, 4575 (1979).

[13] O. G. Ramer and C. H. Wilts, Phys. Status Solidi B **73**, 443 (1976).

[14] X. Jia, K. Liu, K. Xia, and G. E. W. Bauer, Europhys. Lett. **96**, 17 005 (2011).

[15] C. Burrowes, B. Heinrich, B. Kardasz, E. A. Montoya, E. Girt, Y. Sun, Y. Song, and M. Wu, Appl. Phys. Lett. **100**, 092403 (2012).

[16] D. Mills and R. Arias, Physica (Amsterdam) **384B**, 147 (2006).

[17] A. G. Gurevich and G. A. Melkov, *Magnetization Oscillations and Waves* (CRC Press, Boca Raton, 1996).

[18] M. D. Stiles and A. Zangwill, Phys. Rev. B **66**, 014407 (2002).

[19] R. E. De Wames, J. Appl. Phys. **41**, 987 (1970).

[20] B. Hillebrands, Phys. Rev. B **41**, 530 (1990).

[21] H. Puszkarski, IEEE Trans. Magn. **9**, 22 (1973).

[22] P. Wigen, Thin Solid Films **114**, 135 (1984).

[23] C. E. Patton, Phys. Rep. **103**, 251 (1984).

[24] B. A. Kalinikos and A. N. Slavin, J. Phys. C **19**, 7013 (1986).

[25] C. W. Sandweg, Y. Kajiwara, K. Ando, E. Saitoh, and B. Hillebrands, Appl. Phys. Lett. **97**, 252504 (2010).

[26] O. Mosendz, J. E. Pearson, F. Y. Fradin, G. E. W. Bauer, S. D. Bader, and A. Hoffmann, Phys. Rev. Lett. **104**, 046601 (2010).

[27] K. Ando, S. Takahashi, K. Harii, K. Sasage, J. Ieda, S. Maekawa, and E. Saitoh, Phys. Rev. Lett. **101**, 036601 (2008).

[28] L. Liu, T. Moriyama, D. C. Ralph, and R. A. Buhrman, Phys. Rev. Lett. **106**, 036601 (2011).